ResearchGate

See discussions, stats, and author profiles for this publication at: https://www.researchgate.net/publication/9004270

Inter-molecular Coiled-coil Formation in Human Apolipoprotein E C-terminal Domain

ARTICLE *in* JOURNAL OF MOLECULAR BIOLOGY · DECEMBER 2003

Impact Factor: 4.33 · DOI: 10.1016/j.jmb.2003.09.059 · Source: PubMed

CITATIONS
69

READS
47

3 AUTHORS, INCLUDING:

Vincent Raussens
Université Libre de Bruxelles
68 PUBLICATIONS **1,921** CITATIONS
SEE PROFILE

Vasanthy Narayanaswami
Children's Hospital Oakland Research Institute
64 PUBLICATIONS **1,925** CITATIONS
SEE PROFILE

Available from: Vincent Raussens
Retrieved on: 25 January 2016

doi:10.1016/j.jmb.2003.09.059 J. Mol. Biol. (2003) 334, 527–539

JMB

Available online at www.sciencedirect.com

SCIENCE DIRECT®

ELSEVIER

Inter-molecular Coiled-coil Formation in Human Apolipoprotein E C-terminal Domain

Nicole Choy[1], Vincent Raussens[2] and Vasanthy Narayanaswami[1]*

[1]*Lipid Biology in Health and Disease Research Group Children's Hospital Oakland Research Institute, 5700 Martin Luther King Jr Way Oakland, CA 94609-1673 USA*

[2]*Structure and Function of Biological Membranes, Free University of Brussels CP-206/2, bd. Du Triomphe B-1050 Brussels, Belgium*

**Corresponding author*

Human apolipoprotein E (apoE) is composed of an N-terminal (NT) domain (residues 1–191) that bears low-density lipoprotein receptor-binding sites, and a C-terminal (CT) domain (residues 210–299), which houses lipoprotein binding and apoE self-association sites. The NT domain is comprised of a four-helix bundle, while the structural organization of the CT domain is not known. Secondary structural algorithms predict that the apoE CT domain adopts an amphipathic α-helical conformation. On the basis of further sequence predictions, we identified a segment (residues 218–266) in the apoE CT domain that bears a high propensity to form a coiled-coil helix, which coincides with the putative lipoprotein-binding surface. An apoE construct bearing residues 201–299 that encompasses the entire CT domain was designed, expressed in *Escherichia coli* and purified by affinity chromatography. Circular dichroism (CD) spectroscopy of the apoE CT domain reveals spectra characteristic of coiled-coil helices, with the ratio of molar ellipticities at 222 nm and 208 nm ($[\theta]_{222}/[\theta]_{208}$) of 1.03. Trifluoroethanol (TFE) stabilized the secondary structure of the apoE CT domain and disrupted coiled-coil helix formation as determined by CD and tryptophan fluorescence analysis. Analytical ultracentrifugation and lysine-specific cross-linking analysis of the apoE CT domain revealed predominant formation of dimeric and tetrameric species in aqueous buffers, and monomeric forms in 50% TFE. Guanidine hydrochloride-induced denaturation studies reveal that, at low concentrations of denaturant, the apoE CT domain maintains the $[\theta]_{222}/[\theta]_{208}$ ratio at ~1.0 and elicits an altered tertiary environment with a shift in oligomeric state towards a dimer, indicative of the role of coiled-coil helix formation in inter molecular interactions. Further, coiled-coil formation is disrupted by protonation below pH 6.0, with a corresponding decrease in Trp fluorescence emission intensity, demonstrating that salt-bridge interactions play a critical role in maintaining the structural integrity of the apoE CT domain. The data support the concept that inter molecular coiled-coil helix formation is an essential structural feature of the apoE CT domain, which likely plays a role in clustering heparin-binding sites and/or sequestering the lipid-binding surface in lipid-free states.

© 2003 Elsevier Ltd. All rights reserved.

Keywords: apolipoprotein E; coiled-coil helices; C-terminal domain; circular dichroism; fluorescence

Introduction

Apolipoprotein (apo) E is a 34 kDa, 299 residue protein that is a critical component of triglyceride-rich lipoproteins and a sub-class of high-density lipoproteins.[1] It is an anti-atherogenic protein that mediates: (i) cellular uptake of remnant lipoprotein particles by acting as a ligand for the low-density lipoprotein (LDL) receptor family; and (ii) cholesterol efflux from macrophages in atherosclerotic lesions. These processes result in reduction of plasma and cellular cholesterol levels,

Abbreviations used: apo, apolipoprotein; CT, C-terminal; GdnHCl, guanidine hydrochloride; NT, N-terminal; TFE, trifluoroethanol.

E-mail address of the corresponding author: vnarayan@chori.org

0022-2836/$ - see front matter © 2003 Elsevier Ltd. All rights reserved.

respectively,[1–3] and in both cases, lipid association of apoE is a key factor in determining its functionality. Impaired lipoprotein association of apoE leads to its rapid clearance from plasma, with secondary effects on cholesterol levels and metabolism in blood.

apoE is composed of two independently folded domains that are linked *via* a protease-sensitive loop: a 22 kDa N-terminal (NT) domain (residues 1–191) that houses the LDL receptor-binding region and has weak lipid-binding capability;[2] and a 10 kDa C-terminal (CT) domain (residues 210–299) that accommodates high-affinity lipid-binding sites and apoE self-association sites.[4–6] Each domain bears a heparin-binding site, located between residues 142 and 147 in the NT domain and between 243 and 272 in the CT domain.[7,8] High-resolution structural analysis of the isolated NT domain of apoE[9] revealed a four-helix bundle of amphipathic α-helices that sequester the hydrophobic side-chains to the protein interior, while exposing the hydrophilic side-chains to the aqueous environment. The helix bundle is held together by a series of inter- and intrahelical salt-bridges and hydrophobic interactions including leucine zipper-like motifs that account for its great stability. The free energy of stabilization of apoE NT domain is ~10 kcal/mol (1 cal = 4.184 J) with a transition midpoint for guanidine hydrochloride (GdnHCl)-induced denaturation of ~2.5 M, similar to that of globular proteins.

The structural organization of the CT domain, however, is poorly understood. It bears a lower free energy of stabilization, comparable to properties of other apolipoproteins.[4] Computer-based sequence algorithms identify a long amphipathic α-helix in the apoE CT domain composed of a class A and a class G* helix.[10,11] Sedimentation equilibrium and C-terminal truncation analyses indicate that residues 267–299 are responsible for apoE self-association, while residues 245–266 determine lipoprotein binding preference.[5,6,12,13] Further, internal deletion of residues 186–222 and C-terminal truncation of residues 273–299 did not affect lipoprotein binding, suggesting that residues 223–272 encompass a substantial portion of the lipoprotein-binding elements.[14] In other studies, truncation of residues 192–299 resulted in reduced lipid-binding affinity.[15]

These studies raise the issue of the structural organization of the apoE CT domain in the absence of lipid surfaces and the status of lipoprotein-binding sites in this state. Towards this objective, the present study explores the molecular architecture of the recombinant lipid-free apoE CT domain encompassing residues 201–299 employing circular dichroism (CD) and fluorescence spectroscopy, and hydrodynamic and cross-linking analyses. Discrete segments were identified in the apoE CT domain that exhibit hallmark features of coiled-coil helices, which possibly play a role in sequestering the lipoprotein-binding sites in an aqueous environment. We suggest that inter molecular coiled-coil helical formation in the CT domain is an essential structural feature of apoE in the lipid-free state.

Results

Computer-based sequence predictions

The two-domain sequence of apoE3 is shown in Figure 1(a). Secondary structure predictions indicate that the apoE CT domain is predominantly helical, consistent with earlier studies,[10] with the residues possibly existing as one long helix. Further *in silico* analysis of the apoE3 sequence was carried out by the MultiCoil program (Figure 1(b)), which locates and distinguishes coiled-coils in proteins.[16] The probability that a given residue forms a coiled-coil helix in the context of its surrounding 21 residue window of amino acid residues is plotted as a function of the position of the amino acid in the primary sequence. According to this prediction, three segments that bear a propensity to form coiled-coil helices in the entire sequence of apoE3 were identified: two located in the NT domain, between residues 54–106 and 136–158, and one in the CT domain, between residues 218 and 266. The segment located in the CT domain appears to have a high coiled-coil propensity, with a probability factor >0.8 for residues 224–250. The NT domain displayed segments with probability factors of ≤ 0.5 for residues 50–160. Other methods such as PairCoils[17] and Coils[18] yielded an overall similar prediction, albeit with different initial register. As our objective was to obtain structural information about the apoE CT domain, we focused on the independently folded structural and functional segment between residues 201 and 299. A construct encompassing apoE (201–299) was designed, bearing a 17 residue extension (MHHHHHHGLVPRGSIDP) at the N-terminal end with a His-tag (referred to as the apoE CT domain) to facilitate isolation and purification. Recombinant apoE CT domain was expressed in *Escherichia coli* and purified by affinity chromatography. SDS-PAGE analysis and reversed-phase HPLC (not shown) reveal the preparation is ~99% pure. Under the conditions employed, the retention time of the apoE CT domain is 36 minutes by analytical HPLC. Mass spectrometric analysis yielded a mass of 13,345 Da, consistent with an expected molecular mass of 13,343 Da.

Examination of the primary sequence of the apoE CT domain reveals segments composed of sequential heptad repeats of amino acid residues (designated by the letters **a** to **g**), with apolar residues generally occurring at positions **a** and **d**, and polar or hydrophilic residues occupying other positions. Based on *in silico* predictions, residues 222–256 of apoE are projected as one helix of a coiled-coil representation, Figure 2. A striking feature that emerges is the alignment of

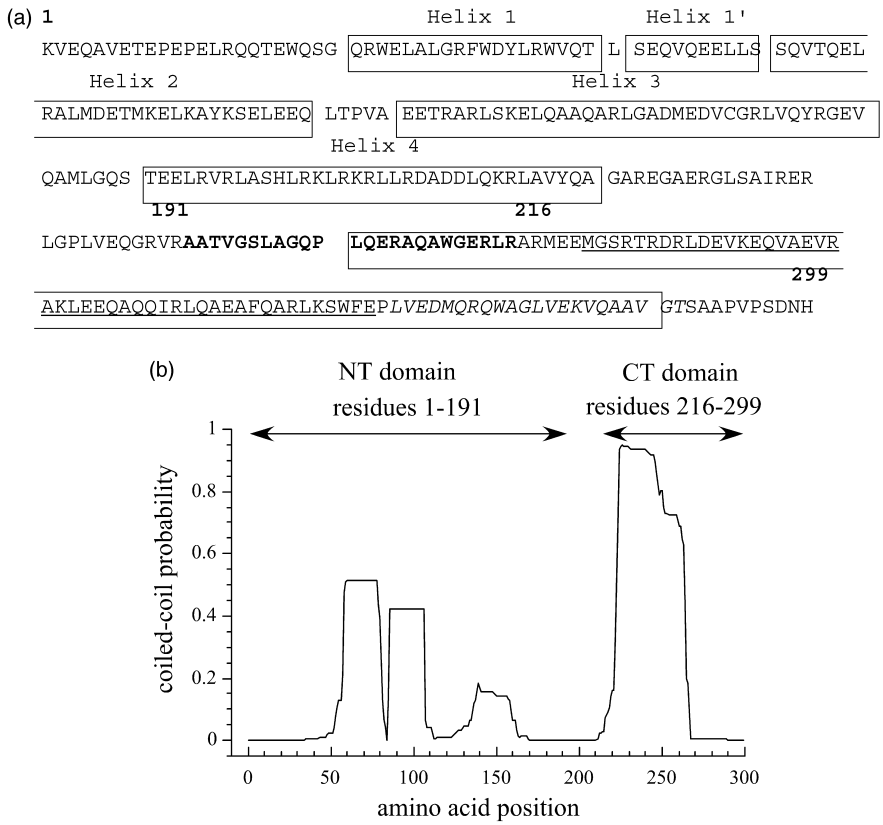

Figure 1. Structural organization of apoE3. (a) Primary sequence and secondary structure organization of human apoE3, which is comprised of an N-terminal domain (residues 1–191) and a C-terminal domain (residues 216–299) separated by a protease-sensitive linker (in bold). Residues involved in the putative lipoprotein-binding site in the CT domain (223–266) are underlined, while residues involved in apoE self-association site (268–289) are shown in italics. Boxes encompass helical segments. In the N-terminal domain, the boundaries of helices were obtained from X-ray analysis of apoE3(1–191).[9] In the rest of the protein, the box comprises residues that are proposed to form an α-helix as predicted by Segrest *et al*.[10] and by a suite of algorithms described on the web site ca.expasy.org. (b) Coiled-coil prediction analysis of apoE3. The predictions are based on a moving 21 residue window surrounding a single residue.[16] The primary sequence position of a residue is indicated on the *X*-axis and the probability scale ranging from 0 to 1 is plotted on the *Y*-axis.

predominantly apolar residues at positions **a** and **d** comprising the putative interhelical interface, which coincides with the proposed lipoprotein-binding surface.[13]

CD analysis

Far-UV CD profile of the apoE CT domain in aqueous buffer reveals troughs at 222 nm and 208 nm (Figure 3, inset), typical of a highly α-helical structure, as reported earlier.[5] The ratio of the molar ellipticities at 222 nm and 208 nm ($[\theta]_{222}/[\theta]_{208}$) has been used as a criterion in several proteins to evaluate the presence of coiled-coil helices. For a non-interacting α-helix, the ratio has been shown to be 0.83,[19] while for two-stranded coiled-coils, the ratio was calculated to be 1.03. In the case of the apoE CT domain, it was calculated to be 1.03, indicative of the presence of coiled-coil helices. The effect of varying the concentration of the apoE CT domain on the $[\theta]_{222}/[\theta]_{208}$ ratio was studied, to evaluate if coiled-coil formation occurs as a result of increasing concentration of protein. The ratio remained unaltered at concentrations ranging from 0.02 mg/ml to 5 mg/ml (Figure 3), suggesting the presence of coiled-coil helices at physiologically relevant levels of apoE. Provencher and Glöckner analysis of the spectra indicates that the α-helical content is about 68%, in good agreement with Fourier transform infrared analysis of the apoE CT domain in aqueous solutions (data not shown) and with structural predictions (both indicating ~70% α-helical content).

Effect of disruption of tertiary interaction by trifluoroethanol (TFE)

To confirm the presence of coiled-coil helices in the apoE CT domain, we rationalized that any environment that disrupts tertiary interactions in proteins will cause coiled-coil helices to exist as non-interacting single helices, an event that can be monitored by CD and fluorescence spectroscopy. The CD spectrum of the apoE CT domain was therefore examined in the presence of various concentrations of TFE (Figure 4(a)). TFE is a

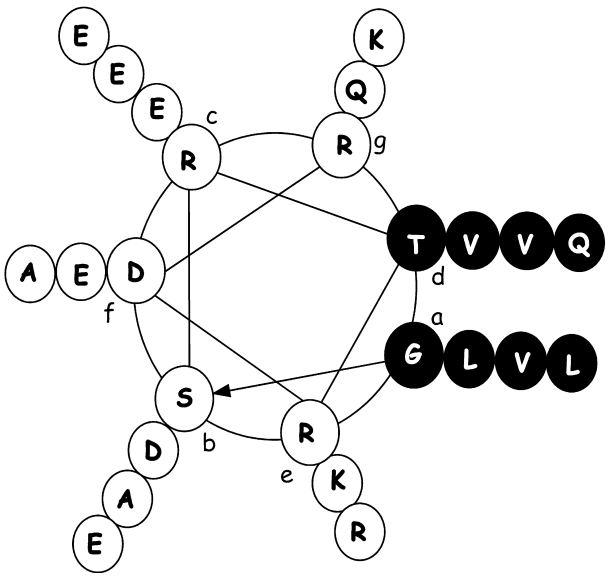

Figure 2. End-on view of apoE residues 222–256 represented as one helix of a coiled-coil. ApoE residues 222–256 are projected in a manner typically employed for representing one helix of a coiled-coil.[62] The view shown is down the helical axis starting with G222 at position **a** in the innermost set of circles, and moving in the direction of the arrow. The residues aligned at positions **a** and **d** are indicated in black circles, while the other positions are shown in white circles.

co-solvent that is known to stabilize secondary structures and disrupt tertiary and quaternary interactions that are stabilized by hydrophobic forces.[20,21] In accordance, an increase in the ellipticity by ~20% was noted upon titration of the

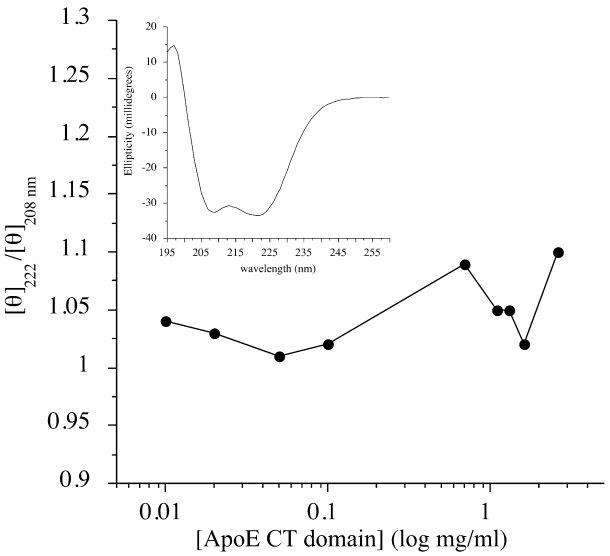

Figure 3. CD analysis of various concentrations of apoE C-terminal domain. Far-UV CD spectra of apoE3 C-terminal domain were recorded in 25 mM potassium phosphate (pH 7.4) at concentrations ranging from 0.01 mg/ml to 2.6 mg/ml and $[\theta]_{222}/[\theta]_{208}$ plotted against log of concentration of the apoE C-terminal domain. The inset shows the CD spectrum of 0.02 mg/ml of the apoE C-terminal domain using a 1 cm path-length cuvette.

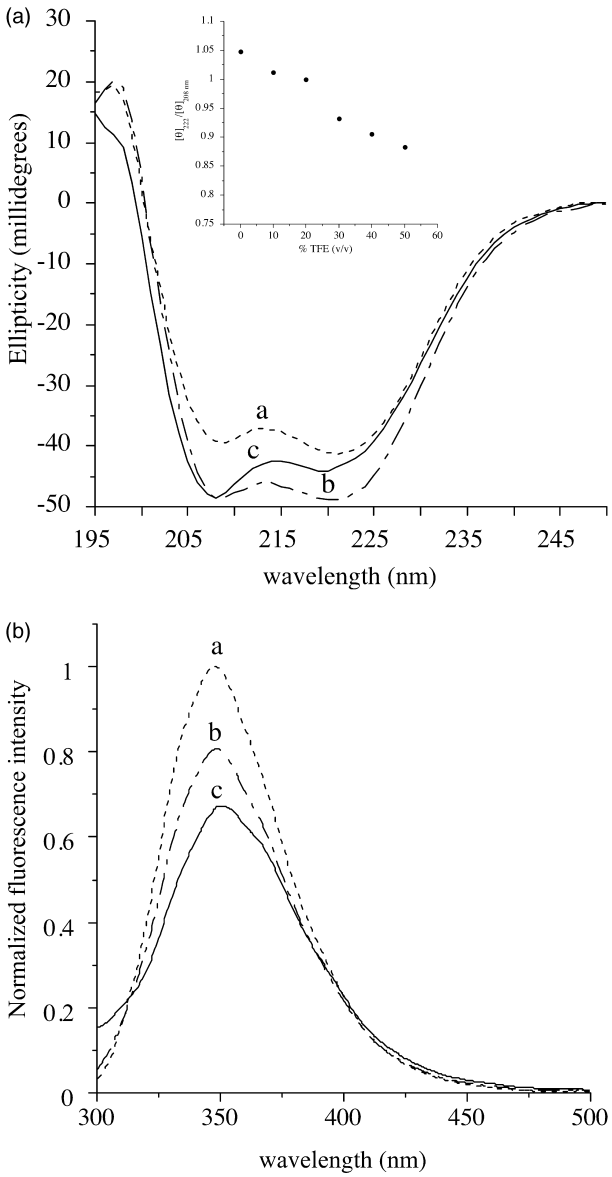

Figure 4. CD and fluorescence spectra of the apoE C-terminal domain in the presence of TFE. CD (a) and fluorescence (b) spectra of 0.1 mg/ml of the apoE C-terminal domain in the presence of various concentrations of TFE: (a) 0%; (b) 20% v/v; (3) 50%. The inset in (a) shows a plot of $[\theta]_{222}/[\theta]_{208}$ *versus* concentration of TFE.

apoE CT domain with up to 20% TFE, with the $[\theta]_{222}/[\theta]_{208}$ ratio remaining at ~1.0 (Figure 4(a), inset). However, at 50% TFE, the $[\theta]_{222}/[\theta]_{208}$ ratio decreased to 0.88, indicative of loss of coiled-coil structure. Further, fluorescence analysis of the apoE CT domain was carried out to assess TFE-induced alterations in the tertiary environment. Fluorescence emission spectra of the apoE CT domain in the absence and the presence of 20% and 50% TFE were recorded (Figure 4(b)). A gradual decrease in fluorescence emission intensity at 348 nm, attributed to Trp residues, was noted with increasing concentration of TFE, with a ~30% decrease in intensity at the maximal

Table 1. Sedimentation equilibrium analysis of apoE CT domain in the presence of 50% TFE

TFE (%)	apoE CT molecular mass (Da)[a]	Best fit
0	43,922	Dimer–tetramer–octamer
50	33,574	Monomer–dimer–tetramer

[a] apoE CT domain was incubated overnight at room temperature in the absence or in the presence of 50% (v/v) TFE. Sedimentation equilibrium analysis was carried out at three different concentrations of apoE CT domain, 0.08, 0.15 and 0.26 mg/ml, at three different rotor speeds each, 16,000, 20,000 and 24,000 rpm. The calculated molecular mass of monomeric apoE CT domain is 13,343 Da.

concentration of TFE studied. The decrease in emission intensity is attributed to quenching of Trp fluorescence as a result of exposure to aqueous environment. Other agents that disrupt tertiary interactions, such as 1% (w/v) SDS or 0.4% (w/v) lysophosphatidylcholine micelles revealed similar trends of behavior characterized by loss of coiled-coil structure (not shown).

To determine if coiled-coil formation is inter- or intramolecular, the oligomeric state of the apoE CT domain was determined by sedimentation equilibrium analysis in the absence and in the presence of 50% TFE (Table 1). An apparent molecular mass of 43,922 Da was obtained from analytical ultracentrifugation experiments of the apoE CT domain in the absence of TFE, consistent with earlier reports.[5,6,12] The data fit best to a model of dimer–tetramer–octomer, with evidence of higher molecular mass species beyond a tetramer resulting from non-specific aggregation rather than a reversible self-association. In the presence of 50% TFE, the data fit best to a monomer-dimer-tetramer model, suggesting that intermolecular interactions in the apoE CT domain have been disrupted considerably by TFE.

In parallel studies, the effect of TFE on the oligomeric state of the apoE CT domain was monitored by chemical cross-linking. Initially, cross-linking was carried out with various concentrations of 3,3′-dithiobis(sulfosuccinimidyl propionate) (DTSSP) for 30 minutes in the absence of TFE (Figure 5A). DTSSP is a thiol-cleavable homobifunctional cross-linker that reacts with the ε-amine group of lysine residues. A band corresponding to the dimeric apoE CT domain appears to be the predominant species (arrow), with smaller amounts of trimers, tetramers and higher molecular mass species appearing at higher concentrations of cross-linker, as shown in previous reports.[6,5] Treatment with reducing agents yielded the monomeric apoE CT domain (not shown), indicating DTSSP-specific cross-linking between spatially proximal lysine residues. In the presence of increasing concentration of TFE (0–50% (v/v), Figure 5B), a corresponding decrease in DTSSP-cross-linked dimer formation was observed.

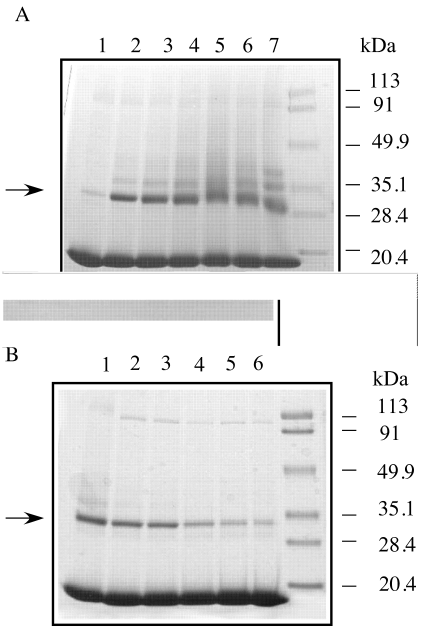

Figure 5. Effect of TFE on cross-linking the apoE C-terminal domain with DTSSP. A, Cross-linking in the absence of TFE as a function of concentration of DTSSP. The apoE C-terminal domain (0.06 mM) was incubated with 0, 0.025, 0.5, 1.0, 5.0, 10 and 20 mM DTSSP (lanes 1–7) at room temperature for 30 minutes in the absence of TFE, followed by addition of 1 M Tris–HCl (pH 7.4) and SDS/4–20% PAGE in the absence of reducing agent. B, Cross-linking in the presence of TFE. The apoE C-terminal domain (0.06 mM) was incubated with 0, 10, 20, 30, 40 and 50% TFE overnight at room temperature followed by addition of DTSSP (0.26 mM) for 30 minutes at room temperature (lanes 1–6). Electrophoresis was carried out as described above. Arrow indicates band corresponding to dimeric apoE CT domain. Protein molecular mass standards are indicated in kDa.

GdnHCl-induced unfolding of the apoE CT domain

Earlier studies demonstrated that the isolated apoE CT domain bears a low free energy of stabilization of ~4 kcal/mol, requiring ~1.0 M GdnHCl to cause 50% denaturation,[4,22] similar to other apolipoproteins.[23–25] In the present study, secondary structural changes associated with unfolding of the apoE CT domain as a function of the concentration of protein and denaturant-induced alterations in the coiled-coil status were evaluated by CD spectroscopy. As the protein concentration increased from 0.02 mg/ml to 2.5 mg/ml, there was a shift in transition mid-point towards higher concentrations of GdnHCl. Representative denaturation profiles at 0.05, 0.1 and 1.6 mg/ml of the apoE CT domain are shown in Figure 6(a). The corresponding mid-points of GdnHCl-denaturation were found to be 0.95, 1.05 and 1.15 M, respectively. Interestingly, an increase in molar ellipticity at 222 nm by ~15% was observed consistently at low concentrations of

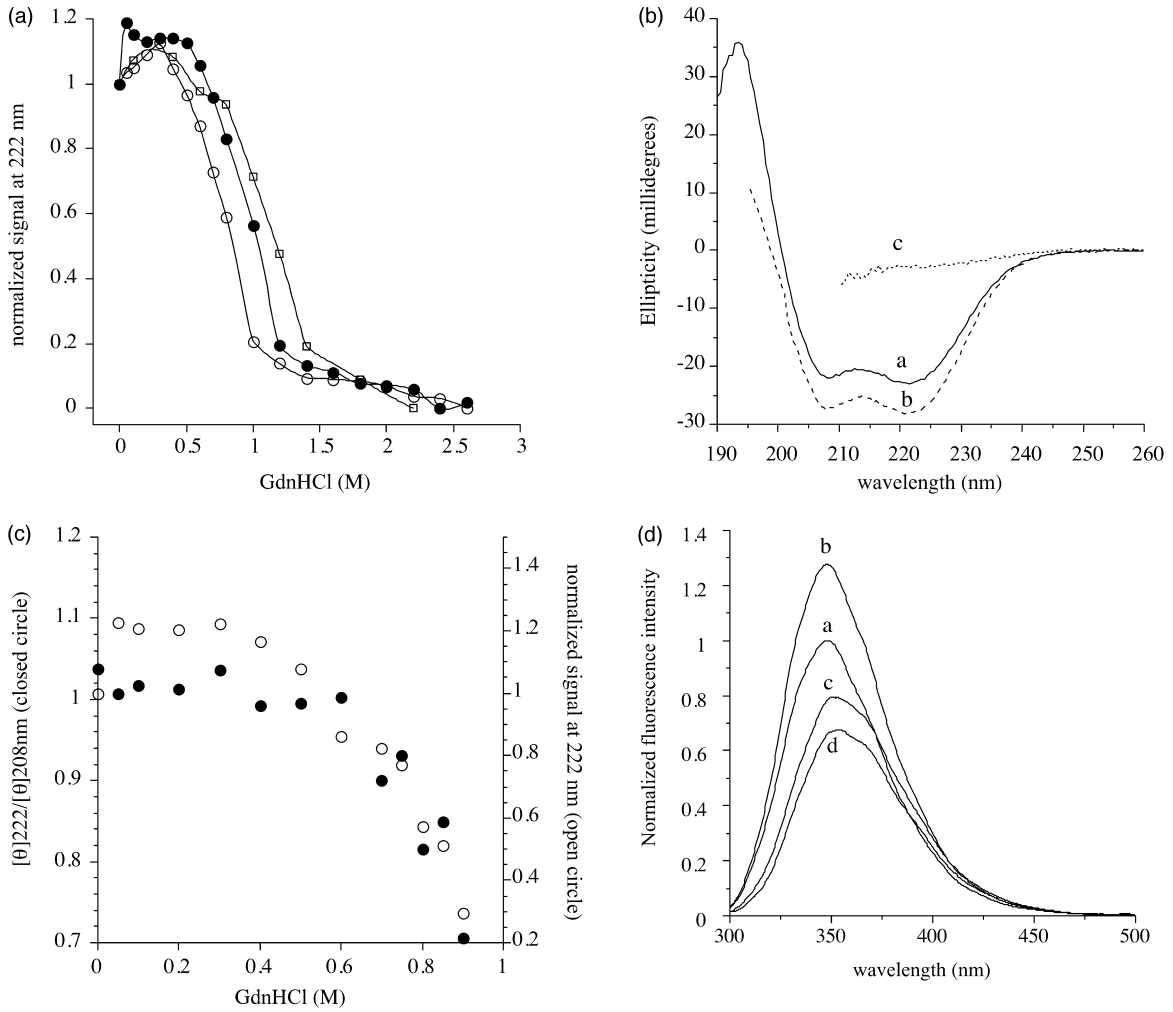

Figure 6. CD analysis of GdnHCl-induced unfolding of the apoE C-terminal domain. (a) Dependence of equilibrium unfolding of the apoE C-terminal domain on concentration of protein. Plot of normalized residue ellipticity at 222 nm as a function of concentration of GdnHCl at the following concentrations of the apoE C-terminal domain: 0.05 mg/ml, open circle; 0.1 mg/ml, filled circle; 1.6 mg/ml, open square. (b) CD spectra of 0.1 mg/ml of the apoE C-terminal domain in 25 mM potassium phosphate (pH 7.4) (0.1 cm path length) in the presence of 0 M (a), 0.3 M (b) and 2.6 M (c) GdnHCl. (c) Plot of $[\theta]_{222}/[\theta]_{208}$ (filled circles) and normalized signal at 222 nm (open circles) *versus* a low concentration of GdnHCl using 0.1 mg/ml of the apoE C-terminal domain. (d) Fluorescence spectra of 0.1 mg/ml of the apoE C-terminal domain in the native state in 25 mM potassium phosphate (pH 7.4) (a), and in the presence of 0.3 M (b), 1.0 M (c) and 2.4 M (d) GdnHCl.

GdnHCl, up to 0.3 M, especially at low concentrations of protein. A pre-transition (negative) slope is generally observed in protein unfolding studies with a small decrease in secondary structural content. The positive slope observed in the case of the apoE CT domain is attributed to the possible stabilizing effect of GdnHCl salt at low concentrations.[26] We noted a similar trend of increased ellipticity when increasing concentrations of NaCl were used, from 0 M to ~0.4 M (data not shown). Further, GdnHCl-induced alteration in the coiled-coil status of the apoE CT domain was assessed. CD spectra of 0.1 mg/ml of the apoE CT domain in the presence of a low concentration (0.3 M) of GdnHCl is depicted in Figure 6(b). Spectra of the native and the completely unfolded apoE CT domain are shown for comparison. Regardless of the increase in ellipticity at 222 nm at low concentrations of GdnHCl, the $[\theta]_{222}/[\theta]_{208}$ ratio was maintained at ~1.0. A plot of $[\theta]_{222}/[\theta]_{208}$ *versus* concentration of GdnHCl (Figure 6(c)) revealed that the ratio is maintained at ~1.0 M up to ~0.4 M GdnHCl, and the decrease in ratio coincides with loss of helical structure during the unfolding process.

In parallel experiments, tertiary structural changes that accompany GdnHCl-induced unfolding were monitored by fluorescence spectroscopy at varying concentrations of protein. Fluorescence emission spectra of 0.1 mg/ml of the apoE CT domain in the native state (0 M GdnHCl) and in the presence of selected concentrations of GdnHCl (0.3, 1.0 and 2.4 M) are shown in Figure 6(d). At 0.3 M GdnHCl, an increase in the fluorescence emission intensity was noted, when compared to the native apoE CT domain, without any change

Table 2. Sedimentation equilibrium and CD analysis of apoE CT domain in the presence of varying concentrations of GdnHCl

GdnHCl (M)	apoE CT molecular mass (Da)[a]	Best fit	$[\theta]_{222}/[\theta]_{208}$[b]
0	42,861	Dimer–tetramer–octamer	1.04
0.05	36,953	Monomer–dimer–tetramer	1.01
0.1	32,850	Monomer–dimer–tetramer	1.02
0.2	29,627	Monomer–dimer–tetramer	1.01
0.3	27,770	Monomer–dimer–tetramer	1.04
1.2	15,263	Monomer–dimer	0.7

[a] For sedimentation equilibrium analysis, apoE CT domain was dialyzed extensively against the indicated concentrations of GdnHCl in 50 mM sodium phosphate (pH 7.0). The analysis was carried out at two different concentrations of apoE CT domain, 0.16 mg/ml and 0.25 mg/ml, at three different speeds each, 16,000, 20,000 and 24,000 rpm.
[b] $[\theta]_{222}/[\theta]_{208}$ was calculated as described in Results.

in the wavelength of maximal Trp emission, suggesting an altered environment for Trp residues. At 1 M GdnHCl there was a decrease in emission intensity accompanied by a red shift in the wavelength of maximal fluorescence emission from 347 nm to 352 nm. In the fully unfolded state at 2.4 M GdnHCl, a further decrease in fluorescence emission intensity occurred. The dependence of GdnHCl-induced unfolding on protein concentration was evaluated by monitoring changes in fluorescence emission intensity (not shown). As protein concentration increased from 0.01 mg/ml to 0.2 mg/ml, there was a shift in mid-point of transition towards higher concentrations of GdnHCl. At a given concentration of protein, GdnHCl-induced mid-point of transition from folded to unfolded state monitored by fluorescence emission coincided with that obtained by CD analysis.

To assess the oligomeric state of the species populating at low concentrations of GdnHCl, sedimentation equilibrium analysis of the apoE CT domain that has been equilibrated with various concentrations of GdnHCl (0, 0.05, 0.1, 0.2, 0.3 and 1.2 M) was performed, Table 2. In the absence of GdnHCl, the molecular mass of the apoE CT domain in 50 mM sodium phosphate (pH 7.0) was 42,861 Da. From 0.05 M to 0.3 M GdnHCl, there was a progressive decrease in molecular mass and the data could be best fit into a monomer–dimer–tetramer model. At 1.2 M GdnHCl, the apoE CT domain was predominantly monomeric, with the best fit to a monomer–dimer model. Parallel studies with increasing concentration of NaCl reveal no changes in the oligomeric state of the apoE CT domain (data not shown). Taken together, CD, fluorescence and analytical ultracentrifugation analysis of the apoE CT domain indicate that the species populating low concentrations of GdnHCl is a dimer, bearing intermolecular coiled-coil helical conformation.

Effect of altering pH

To determine the possible role of electrostatic interactions in maintaining the helical structure and tertiary interactions in the apoE CT domain, the effect of altering the solution pH was monitored by CD and fluorescence spectroscopy (Figure 7). As the pH of the buffer was lowered from 6.0, there was a striking display of decrease in Trp fluorescence emission, concomitant with loss of helical structure, with about 50% residual signal retained between 4.5 and 5.0. The $[\theta]_{222}/[\theta]_{208}$ value remained at ~1.0 only between pH 6.0 and 9.5, with a loss in coiled-coil helical structure noted at pH <6.0.

Discussion

Coiled-coil helices are frequently encountered motifs in protein–protein interactions involving subunit oligomerization.[27–29] They are of significant structural and functional importance, offering highly specific means of protein–protein interaction to maintain the inter-molecular interface. Studies on two-stranded coiled-coil motifs that are localized in fibrous proteins and eukaryotic

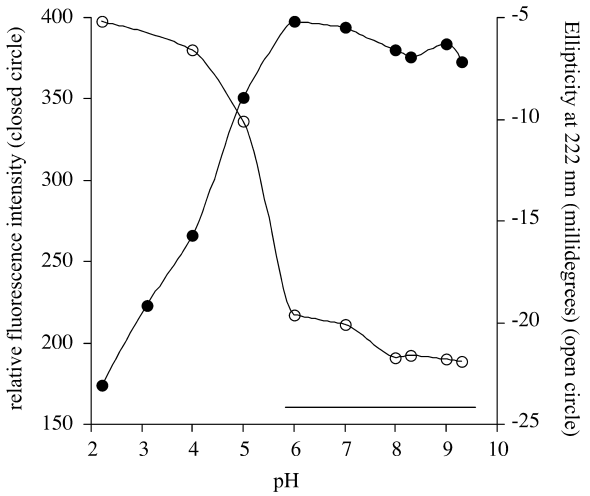

Figure 7. pH-dependence of the apoE C-terminal domain helical structure and Trp fluorescence emission. CD and fluorescence emission spectra of 0.1 mg/ml of the apoE C-terminal domain were recorded as described for Figure 6, at various pH values. The relative fluorescence intensity of Trp emission (filled circles) and the millidegrees at 222 nm (open circles) are plotted as a function of pH. The line indicates the pH at which the $[\theta]_{222}/[\theta]_{208}$ remains at ~1.0.

transcription factors have offered valuable insights into the fundamentals of protein folding and stability.

The occurrence of apolar residues at the **a** and **d** positions of tandem heptad repeats is a hallmark feature of coiled-coil α-helices, where the hydrophobic residues form the interface between the helices and pack in a regular pattern along a dimerization surface.[30–32] Algorithms designed to predict the occurrence of coiled-coil α-helices on the basis of known protein structures indicate that the apoE sequence has segments with a propensity to form such tertiary interactions. We applied the method of MultiCoil,[16] a program based on PairCoils,[17] that analyzes the relative frequency of occurrence of amino acid residues at each position of the heptad repeat. In the case of the apoE NT domain, X-ray crystal analysis of apoE3(1–191) reveals the occurrence of leucine residues at every seventh position on adjacent anti-parallel helices that stabilize interfaces between helix 1 and helix 4, and between helix 2 and helix 3.[9] This observation is consistent with *in silico* predictions of the apoE NT domain, although the overall coiled-coil score was lower for this segment. Nevertheless, the concurrence of the predictions with high-resolution analysis validates the reliability of the MultiCoil algorithm. In the case of the apoE CT domain, these methods predict a higher probability of coiled-coil helix formation. While the coiled-coil motif is intra-molecular in the NT four-helix bundle of apoE3, we propose that inter-molecular coiled-coil formation occurs in CT domain, with the **a** and **d** positions occupied predominantly by hydrophobic residues. Examination of this segment of apoE from different mammalian species revealed that the coiled-coil propensity is conserved (not shown), suggesting an important role for this region. Interestingly, the heptad repeat in the CT domain is interrupted by a "stutter" between residues Q246 (d) and A247 (A), as shown below, the significance of which is unclear:

```
222                                                  264
GSRTRDRLDEVKEQVAEVRAKLEEQAQQIRLQAEAFQARLKSW
a  d  a  d  a  d  a  dA  d  a  d  a  d
```

To avoid possible contribution from the NT domain, which may complicate our interpretation, we employed the isolated apoE CT domain encompassing residues 201–299 for our investigation. The recombinant apoE CT domain has the expected molecular mass and retains the overall structural and solution behavior of the apoE CT domain comprising residues 216–299, generated by treatment of intact apoE with thrombin.[4,5] Secondary structure predictions indicate that residues 202–287 have a propensity to form an amphipathic α-helix (residues 200–266, class A helix; residues 270–290, class G* helix),[10] although algorithms for coiled-coil helices predict that residues 223–264 have a probability factor >0.5 of forming coiled-coil helices. It is likely that residues outside 223–264 may play a role in maintaining the coiled-coil status of this segment. Whereas the isolated apoE CT domain retains all the functional properties and is an independently folded structural unit, peptide fragments encompassing discrete segments of this domain such as apoE 202–243, 211–243,[33] 263–286 and 267–286,[33,34] remain unstructured (and monomeric) in aqueous solutions. Therefore, we found it essential to maintain the entire CT domain intact in order to obtain better insight into its organization in the lipid-free state. Further, it was important to retain the structural elements of the critical lipid-binding surface[8] contained in residues 223–272 and self-association sites between 267 and 299.[13] As an exchangeable apolipoprotein exhibiting reversible lipid-binding capability, it is most likely that lipid-associated apoE is in equilibrium with lipid-free apoE.[6] Whereas lipid-association is an essential prerequisite for apoE function, several studies reveal the physiological and pathological relevance of lipid-free apoE and its fragments,[35–38] for which precise conformational information is lacking.

Earlier studies indicate that the isolated apoE CT domain has a high α-helical content,[5] and causes apoE self-association in the absence of lipids, forming tetramers and higher-state oligomers. Using the coiled-coil prediction as a premise, we carried out additional CD analysis on the apoE CT domain to further understand the helical organization of this domain. The $[\theta]_{222}/[\theta]_{208}$ ratio in the CD spectrum of α-helical proteins displaying characteristic troughs has been used generally as an indicator of coiled-coil formation. The difference between absorbance at 208 nm and at 222 nm has been attributed to the amide $\pi-\pi^*$ electronic transition band at 208 nm, which polarizes parallel with the helical axis and is sensitive to whether an α-helix is single-stranded or is interacting with another helix such as a two-stranded coiled-coil. Whereas the molar ellipticity at 222 nm, corresponding to the amide $\pi-\pi^*$ electronic transition, remains unchanged during this inter-helical interaction, decreased values of molar ellipticity at 208 nm are noted upon formation of a two-stranded coiled-coil.[39] Thus, the $[\theta]_{222}/[\theta]_{208}$ ratio has generally been used to distinguish between coiled-coil helices (ratio of 1.0 ± 0.03) and non-associated helices (ratio between 0.8 and 0.9),[20,40–44] although in limited examples of synthetic polypeptides that do not form coiled-coils, a ratio of 1.0 has been reported.[45,46] In the case of the apoE CT domain, a ratio of 1.0 was noted consistently at all concentrations studied, including 10 μg/ml, suggesting that coiled-coil helix formation is an essential structural element in maintaining protein–protein interaction. The apoE CT domain exhibits a $[\theta]_{222}/[\theta]_{208}$ ratio of 1.0 at low concentrations (~35 μg/ml) where apoE has been demonstrated to exist as a dimer.[12] This observation suggests that

intermolecular coiled-coil helix formation is an important structural feature for apoE self-association. The predominant occurrence of dimeric species when treated with DTSSP supports this observation. Lysine residues at **e** and **g** positions from participating helices (Figure 2) are likely involved in the cross-linking reaction.

With increasing amounts of TFE, the coiled-coil nature of the apoE CT domain was gradually lost, as indicated by a decrease in $[\theta]_{222}/[\theta]_{208}$ ratio, and a corresponding increase in α-helical content was observed. The increase in helical content likely reflects TFE-induced transformation of loops and disordered segments to α-helices, potentially forming an extended α-helix. Further, fluorescence analysis indicates a progressive decrease in Trp fluorescence emission with increasing concentrations of TFE, indicative of exposure to aqueous environment. There was no evidence of intermolecular cross-linking in the apoE CT domain in the presence of TFE. Taken together with analytical ultracentrifugation analysis, these data support the concept of a prevalence of monomeric species of the apoE CT domain in the presence of TFE. The observed changes possibly represent replacement of protein–protein interactions by protein–TFE interactions, as TFE is known to disrupt tertiary and quaternary interactions, while stabilizing and increasing secondary structure in proteins.[19,20] It is envisaged that TFE induces conformational changes reminiscent of those induced by lipids.[47]

GdnHCl-induced unfolding of the apoE CT domain revealed interesting aspects of the structural organization of the protein. The increase in molar ellipticity (~20%) without changes in $[\theta]_{222}/[\theta]_{208}$ ratio noted at low concentrations of GdnHCl, likely represents dissociation of tetrameric apoE to dimeric forms, which in turn is maintained by coiled-coil helix formation. The increase in ellipticity at 222 nm possibly reflects conversion of loop and/or unstructured segments to α-helical conformation as a result of the stabilizing effect of low concentrations of GdnHCl on protein structure.[48,49] Kohn *et al*.[48] demonstrated a striking example with a 35-mer peptide, wherein GdnHCl induced helical structure at low concentrations, possibly by a combination of general electrostatic charge screening and through hydrogen bonding. The electrostatic charge screening may mask positive charge repulsions by the chloride ions of GdnHCl, or mask negative charge repulsions by the guanidinium ions; at high concentrations GdnHCl acts as a denaturant.[50] NaCl, on the other hand, is non-denaturing and causes similar response in secondary structure only at low concentrations. In the case of the apoE CT domain, the **e** and **g** positions flanking the hydrophobic **a** and **d** positions are occupied predominantly by positively charged residues (Figure 2). This occurrence may cause inter-helical electrostatic repulsion leading to a low level of protein stability, which bears possible functional implications, facilitating helix–helix interactions of the apoE CT domain in the lipid-free state to be replaced by helix–lipid interactions during lipid association.

The secondary structural changes are accompanied by increased Trp emission, which may be explained by tertiary structural alterations in the vicinity of Trp residues resulting in an increased hydrophobic environment. Similar denaturant-induced increase in fluorescence emission of Trp has been noted in initial stages of unfolding of bacterial luciferase, a heterodimeric protein, in which the tryptophan residues remained buried at lower concentrations of urea.[51] Trp264 is a potential candidate in the apoE CT domain that reports on the observed tertiary changes, as it is located at the interface between the putative coiled-coil and type G* helical segments. In conjunction with sedimentation equilibrium analysis at low concentrations of GdnHCl, which reveal a shift in equilibrium towards a dimeric state, CD and fluorescence data indicate dissociation of the tetrameric protein to a dimeric state likely constitutes the initial step of unfolding.

On the basis of these observations, we propose that residues 218–266 of adjacent apoE molecules form a coiled-coil homodimer, which upon juxtaposition with a neighboring dimer promotes a four-helix bundle formation in residues 267–299. Two likely models of the apoE CT domain organization are represented in Figure 8, with the helices oriented either parallel with or anti-parallel to each other. At this juncture, it is not clear if residues 218–266 alone form a coiled-coil helix (as suggested by computer-based predictions) or if the entire segment spanning up to position 299 is involved. Further, since GdnHCl-induced transitions as monitored by CD and fluorescence spectral probes are superimposable, it is likely that loss of coiled-coil structure results in a rapid collapse of the protein, suggesting that coiled-coil formation is an essential structural feature in the apoE CT domain in aqueous solutions. In addition, the sharp decline in helical structure and Trp fluorescence emission, in conjunction with loss of coiled-coil structure as a result of protonation (beyond the theoretical pI of the construct, ~6.4) is indicative of critical electrostatic interactions in maintaining the structural integrity of the apoE CT domain. Charged residues contribute to 29% of the total amino acid residues in the apoE CT domain construct, with 18 acidic and 16 basic residues within salt-bridge-forming distance of each other (i, $i+4$ sequence configuration).

Coiled-coil formation likely facilitates clustering of positively charged residues that mediate heparin binding in the lipid-free apoE CT domain between residues 243 and 272.[2,7] In a recent study, Lys233 (located in the center of the proposed coiled-coil segment), was indicated to possess an unusually basic microenvironment, with tetramerization *via* the CT domain considered an essential aspect to elicit heparin-binding ability.[52] In the case of apoE7, a naturally occurring mutant in the human population, where Glu244 and Glu245 are each

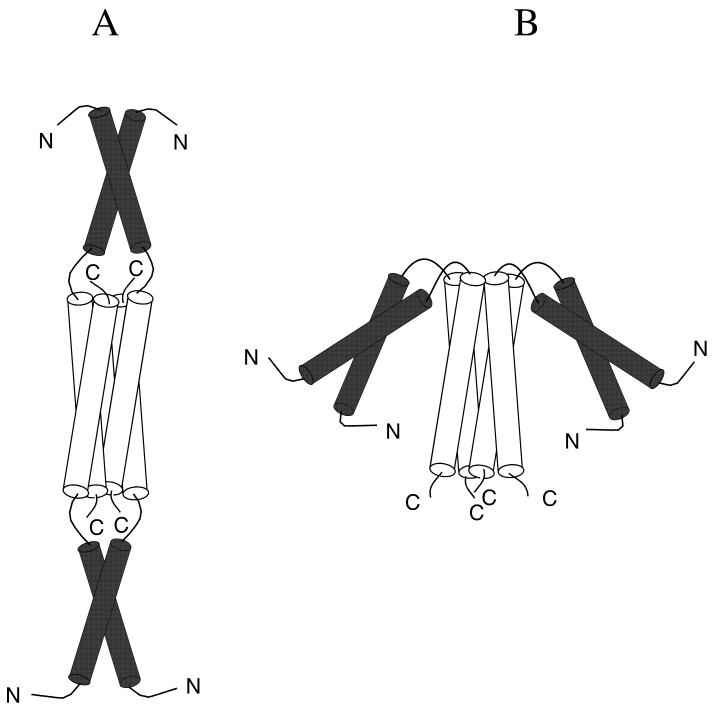

Figure 8. A model of the lipid-free helical organization of the apoE C-terminal domain. The tetrameric apoE CT domain is modeled as a dimer of dimers. Two possible models of helical organization are represented with the self-associating site (white cylinders) as two pairs of helices aligned anti-parallel (left) or parallel (right) to each other. The putative inter-molecular coiled-coil helices are shown as black cylinders.

replaced by a lysine residue, a higher binding affinity for heparin and preferential association with very low-density lipoproteins (VLDL) was demonstrated.[8] The authors' suggestion that the mutations stabilize a long helix, which in turn is better accommodated on lipoproteins with small radius of curvatures such as VLDL, may be extended to include stabilization of a coiled-coil helix. Further, the loss of heparin binding of both wild-type apoE3 and apoE7 upon lipid association supports the concept that protein dissociation is coupled to lipid binding.

The protein concentration dependence of unfolding has been used as a determining feature of dissociation coupled to denaturation.[53,54] We propose that the solution behavior of the apoE CT domain follows the scheme

$$\text{tetramer} \leftrightarrow \text{dimer} \leftrightarrow \text{monomer}$$

in equilibrium with partially and fully denatured intermediate and monomeric states. At ~1 M GdnHCl, the transition likely involves the monomeric apoE CT domain, as suggested in other studies involving extrinsically labeled intact apoE.[55] These authors suggest an equilibrium scheme involving "closed" tetramer ↔ "open" tetramer ↔ native or partially denatured monomer ↔ fully denatured monomer, on the basis of fluorimetric, chromatographic and immunochemical studies, with a dimeric intermediate detected in cross-linking analysis.[56]

Initial crystallographic analysis of apoE (223–272) by Weisgraber and co-workers[57] indicates the putative presence of a dimer as suggested by a weak non-crystallographic symmetry axis relating two α-helices packing at an angle of ~20°. Such an arrangement is observed in packing of ridges of a helix into grooves of another for coiled-coil helices.[58] The region examined by these authors corresponds to the proposed coiled-coil segment in the present study, further supporting our conclusions. In apoE, the relative stabilities of the NT and CT domains appear to be inversely related to their lipid-binding abilities, a mechanism proposed to play a physiological role in conferring receptor-binding activity to the former, with the entire protein anchored *via* the CT domain.[59] Although a commonly occurring motif, the coiled-coil formation in the apoE CT domain likely represents a novel structural feature identified in apolipoproteins, providing a mechanism that facilitates sequestration of hydrophobic residues in the lipid-free state, which become available for lipid interaction upon encountering an appropriate lipoprotein surface.

Materials and Methods

Materials

Trifluoroethanol (TFE) and lysophosphatidyl choline were obtained from Sigma (St Louis, MO). Cross-linkers disuccinimidyl suberate (DSS) and 3,3′-dithiobis-(sulfosuccinimidyl propionate) (DTSSP) were obtained from Pierce Biotechnology (Rockford, IL). Ultra-pure guanidine hydrochloride was purchased from ICN Biomedicals, Inc. (Aurora, OH).

Expression and purification of recombinant apoE CT domain

A pET22b expression vector encoding apoE (201–299) and bearing a His-tag at the N-terminal end was constructed. DNA sequencing was performed to confirm

the sequence. The recombinant wild-type apoE CT domain was expressed in *E. coli* and recovered by affinity chromatography on a Ni-affinity matrix (HiTrap™ chelating column, Amersham Pharmacia Biotech). Typical yields of protein were ~5 mg/l of culture, with ~99% purity as estimated from analytical reversed-phase HPLC on a Zorbax RX-C8 (150 mm × 2.1 mm i.d. 5 μm particle size) column. The flow-rate was 2 ml/minute with a linear AB gradient, where eluent A is aqueous 0.05% trifluoroacetic acid (TFA) and eluent B is 0.05% TFA in acetonitrile (2% acetonitrile/minute). Molecular mass determination was carried out on LC-Ion Trap mass spectrometer (Esquire 3000plus) (Bruker Daltonics, Fremont, CA).

GdnHCl-induced equilibrium unfolding

Stock solutions of GdnHCl and the apoE CT domain were prepared in 25 mM potassium phosphate (pH 7.0), mixed to the final concentrations indicated and incubated overnight at room temperature. The final concentration of GdnHCl ranged from 0 M to 2.6 M. Secondary structural changes that accompany GdnHCl-induced unfolding were monitored by CD spectroscopy on an Applied Photophysics PiStar-180 spectrometer (Leatherhead, UK) at room temperature. CD spectra were obtained by collecting data at 0.5 nm intervals from 260 nm to 190 nm and averaged over 20,000 points. Cuvettes of various path-lengths (0.02, 0.1, and 1 cm) were employed. Values depicted are representative of five individual experiments. The molar ellipticity ([θ]) in deg cm^2 dmol^{-1} at 222 nm or 208 nm was calculated from the equation:

$$[\theta] = \mathrm{MRW}\theta/10dc$$

where MRW is the mean residue weight of the apoE CT domain calculated to be 115.03, θ is the measured ellipticity in degrees at 222 nm or 208 nm, d is the cuvette path-length (in cm) and c is the protein concentration (in g/ml). Thermodynamic calculations were not carried out, given the complex nature of the unfolding process. The unfolding process was examined by monitoring the fluorescence emission of tryptophan (Trp), following excitation at 280 nm. The excitation and emission slit-widths were set at 3 nm and the spectra were recorded between 300 nm and 500 nm on a Perkin–Elmer spectrofluorimeter at room temperature. The apoE CT domain contains three Trp residues, at positions 210, 264 and 276 (and no Tyr residue), which were used as probes of tertiary interactions in the protein. Trp210 is located close to the N-terminal end preceding the putative coiled-coil segment; Trp264 is predicted to be close to the C-terminal end of the proposed coiled-coil segment, while Trp276 is located in the proposed interface for oligomerization. A blank spectrum of buffer alone was subtracted from all spectra.

Effect of trifluoroethanol

A sample (50 μg) of the apoE CT domain was incubated overnight at room temperature in the absence or in the presence of various concentrations of TFE, ranging from 10% to 50% (v/v). CD and fluorescence measurements were carried out on these samples as described above.

Sedimentation equilibrium analysis

Sedimentation equilibrium experiments were carried out in a Beckman XL-1 analytical ultracentrifuge at 20 °C using absorbance optics.[60] Data were recorded at three different concentrations of protein at 14,000 rpm and 18,000 rpm, and each speed maintained until equilibrium was attained (there were no significant differences in $r^2/2$ *versus* absorbance scans recorded two hours apart). Sedimentation equilibrium data were evaluated by the NONLIN program, which incorporates a non-linear, least-squares curve-fitting algorithm.[61]

Cross-linking analysis

Cross-linking experiments were carried out using the water-soluble cross-linker DTSSP. Reaction mixtures contained 0.5–1.0 mg/ml of the apoE CT domain and various concentrations of DTSSP in 25 mM phosphate (pH 7.4) in the absence or the presence of 50% TFE. Incubations were carried out for 30 minutes at room temperature. The reaction was quenched by the addition of 1 M Tris (pH 7.4) and/or non-reducing SDS-PAGE sample treatment buffer for 15 minutes. As the cross-linker is cleavable by thiols, samples were treated with either reducing or non-reducing SDS-PAGE sample treatment buffer, to confirm cross-linking. In other studies, DSS was employed as the cross-linking agent under identical conditions, with the exception that DMSO was used as the solvent for DSS at concentrations not exceeding 2% (v/v) of total reaction mixtures.

Effect of altering pH

To determine the pH-dependency of the apoE CT domain helical structure and tertiary interactions, the protein was incubated overnight in 20 mM sodium acetate, sodium phosphate or Tris buffer at the desired pH at 4 °C. CD and fluorescence measurements were carried out at room temperature as described above.

Secondary structure and coiled-coil helix predictions

Secondary structure predictions of apoE CT domain were carried out as described on the web†. The sequence was further analyzed by the MultiCoil program, which predicts the location of coiled-coil segments in proteins[15] and the probability that a sequence of amino acid residues forms a coiled-coil helix. The prediction for any given residue is based on the amino acid residues in a 21 residue window surrounding that residue.

Acknowledgements

The authors thank Dr Cyril Kay and Les Hicks for sedimentation ultracentrifugation analyses, and Dr Xinyi Zhang for mass spectrometric analysis. This work was supported by an American Heart Association grant to V.N.

† http://ca.expasy.org

References

1. Mahley, R. W. (1988). Apolipoprotein E: cholesterol transport protein with expanding role in cell biology. *Science*, **240**, 622–630.
2. Weisgraber, K. H. (1994). Apolipoprotein E: structure-function relationships. *Advan. Protein Chem.* **45**, 249–302.
3. Von Eckardstein, A., Nofer, J.-R. & Assmann, G. (2001). High density lipoproteins and arteriosclerosis. Role of cholesterol efflux and reverse cholesterol transport. *Arterioscler. Thromb. Vasc. Biol.* **21**, 13–27.
4. Wetterau, J. R., Aggerbeck, L. P., Rall, S. C., Jr & Weisgraber, K. H. (1988). Human apolipoprotein E3 in aqueous solutions II. Evidence for two structural domains. *J. Biol. Chem.* **263**, 6240–6248.
5. Aggerbeck, L. P., Wetterau, J. R., Weisgraber, K. H., Wu, C.-S. C. & Lindgren, F. T. (1988). Human apolipoprotein E3 in aqueous solution. II. Properties of the amino- and carboxyl-terminal domains. *J. Biol. Chem.* **263**, 6249–6258.
6. Yokoyama, S., Kawai, Y., Tajima, S. & Yamamoto, A. (1985). Behavior of human apolipoprotein E in aqueous solutions and at interfaces. *J. Biol. Chem.* **260**, 16375–16382.
7. Weisgraber, K. H., Rall, S. C., Jr, Mahley, R. W., Milne, R. W., Marcel, Y. L. & Sparrow, J. T. (1986). Human apolipoprotein E. Determination of the heparin binding sites of apolipoprotein E3. *J. Biol. Chem.* **261**, 2068–2076.
8. Dong, J., Balestra, M. E., Newhouse, Y. M. & Weisgraber, K. H. (2000). Human apolipoprotein E7: lysine mutations in the carboxy-terminal domain are directly responsible for preferential binding to very low-density lipoproteins. *J. Lipid Res.* **41**, 1783–1789.
9. Wilson, C., Wardell, M. R., Weisgraber, K. H., Mahley, R. W. & Agard, D. A. (1991). Three-dimensional structure of the LDL receptor-binding domain of human apolipoprotein E. *Science*, **252**, 1817–1822.
10. Segrest, J. P., Jones, M. K., DeLoof, H., Brouillette, C. G., Venkatachalapathi, M. & Anantharamaiah, G. M. (1992). The amphipathic helix in the exchangeable apolipoproteins: a review of secondary structure and function. *J. Lipid Res.* **33**, 141–166.
11. De Pauw, M., Vanloo, B., Dergunov, A. D., Devreese, A.-M., Baert, J., Brasseur, R. & Rosseneu, M. (1997). Composition and structural and functional properties of discoidal and spherical phospholipid–apoE3 complexes. *Biochemistry (Moscow)*, **62**, 251–263.
12. Perugini, M. A., Schuck, P. & Howlett, G. J. (2000). Self-association of human apolipoprotein E3 and E4 in the presence and absence of phospholipids. *J. Biol. Chem.* **275**, 36758–36765.
13. Westerlund, J. A. & Weisgraber, K. H. (1993). Discrete carboxyl-terminal segments of apolipoprotein E mediate lipoprotein association and protein oligomerization. *J. Biol. Chem.* **268**, 15745–15750.
14. Dong, L.-M., Wilson, C., Wardell, M. R., Simmons, T., Mahley, R. W., Weisgraber, K. H. & Agard, D. A. (1994). Human apolipoprotein E: role of arginine 61 in mediating the lipoprotein preferences of the E3 and E4 isoforms. *J. Biol. Chem.* **269**, 22358–22365.
15. Gillotte, K. L., Zaiou, M., Lund-Katz, S., Anantharamaiah, G. M., Holvoet, P., Dhoest, A. *et al.* (1999). Apolipoprotein-mediated plasma membrane microsolubilization. Role of lipid affinity and membrane penetration in the efflux of cellular cholesterol and phospholipid. *J. Biol. Chem.* **274**, 2021–2028.
16. Wolf, E., Kim, P. S. & Berger, B. (1997). MultiCoil: a program for predicting two- and three-stranded coiled-coils. *Protein Sci.* **6**, 1179–1189.
17. Berger, B., Wilson, D. B., Wolf, E., Tonchev, T., Milla, M. & Kim, P. S. (1995). Predicting coiled-coils by use of pairwise residue correlations. *Proc. Natl Acad. Sci. USA*, **92**, 8259–8263.
18. Lupas, A. (1996). Prediction and analysis of coiled-coil structures. *Methods Enzymol.* **266**, 513–525.
19. Zhou, N. E., Kay, C. M. & Hodges, R. S. (1992). The two-stranded alpha-helical coiled-coil is an ideal model for studying protein stability and subunit interactions. *J. Biol. Chem.* **267**, 2664–2670.
20. Lau, S. Y. M., Taneja, K. & Hodges, R. S. (1984). Synthesis of a model protein of defined secondary and quaternary structure. *J. Biol. Chem.* **259**, 13253–13261.
21. Frère, V., Sourgen, F., Monnot, M., Troalen, F. & Fermandjian, S. (1995). A peptide fragment of human DNA topoisomerase II alpha forms a stable coiled-coil structure in solution. *J. Biol. Chem.* **270**, 17502–17507.
22. Morrow, J. A., Segall, M. L., Lund-Katz, S., Phillips, M. C., Knapp, M., Rupp, B. & Weisgraber, K. H. (2000). Differences in stability among the human apolipoprotein E isoforms determined by the amino-terminal domain. *Biochemistry*, **39**, 11657–11666.
23. Sparks, D. L., Lund-Katz, S. & Phillips, M. C. (1992). The charge and structural stability of apolipoprotein A-I in discoidal and spherical recombinant high-density lipoprotein particles. *J. Biol. Chem.* **267**, 25839–25847.
24. Weinberg, R. B. & Spector, M. S. (1985). The self-association of human apolipoprotein A-IV. Evidence for an *in vivo* circulating dimeric form. *J. Biol. Chem.* **260**, 4914–4921.
25. Gursky, O. & Atkinson, D. (1998). Thermodynamic analysis of human plasma apolipoprotein C-1: high-temperature unfolding and low-temperature oligomer dissociation. *Biochemistry*, **37**, 1283–1291.
26. Ibarra-Molero, B., Loladze, V. V., Makhatadze, G. I. & Sanchez-Ruis, J. (1999). Thermal *versus* guanidine-induced unfolding of ubiquitin. An analysis in terms of the contributions from charge–charge interactions to protein stability. *Biochemistry*, **38**, 8138–8149.
27. Cohen, C. & Parry, D. A. D. (1990). Alpha-helical coiled-coils and bundles: how to design an α-helical protein. *Proteins: Struct. Funct. Genet.* **7**, 1–15.
28. Lupas, A. (1996). Coiled-coils: new structures and new functions. *Trends Biochem. Sci.* **21**, 375–382.
29. Kohn, W. D., Mant, C. T. & Hodges, R. S. (1997). Alpha-helical protein assembly motifs. *J. Biol. Chem.* **272**, 2583–2586.
30. Hodges, R. S., Sodek, J., Smillie, L. B. & Jurasek, L. (1972). Tropomyosin: amino acid sequence and coiled-coil structure. *Cold Spring Harbor Symp. Quant. Biol.* **37**, 299–310.
31. Cohen, C. & Parry, D. A. D. (1994). Alpha-helical coiled-coils: more facts and better predictions. *Science*, **263**, 488–489.
32. Tarbouriech, N., Curran, J., Ruigrok, R. W. H. & Burmeister, W. P. (2000). Tetrameric coiled-coil domain of Sendai virus phosphoprotein. *Nature Struct. Biol.* **7**, 777–781.
33. Sparrow, J. T., Sparrow, D. A., Fernando, G., Culwell, A. R., Kovar, M. & Gotto, A. M., Jr (1992). Apolipoprotein E: phospholipid binding studies with synthetic peptides from the carboxyl terminus. *Biochemistry*, **31**, 1065–1068.

34. Wang, G., Pierens, G. K., Treleaven, W. D., Sparrow, J. T. & Cushley, R. J. (1996). Conformations of human apolipoprotein E (263–286) and E (267–289) in aqueous solutions of sodium dodecyl sulfate by CD and 1H NMR. *Biochemistry*, **35**, 10358–10366.
35. Narita, M., Holtzman, D. M., Fagan, A. M., LaDu, M. J., Yu, L., Han, X. *et al.* (2002). Cellular catabolism of lipid poor apolipoprotein E *via* cell surface LDL receptor-related protein. *J. Biochem.* **132**, 743–749.
36. Cho, H. S., Hyman, B. T., Greenberg, S. M. & Rebeck, G. W. (2001). Quantifications of apoE domains in Alzheimer's disease brain suggests a role for apoE in Aβ aggregation. *J. Neuropathol. Expt.* **60**, 342–349.
37. Huang, Y., Liu, X. Q., Wyss-Coray, T., Brecht, W. J., Sanan, D. A. & Mahley, R. W. (2001). Apolipoprotein E fragments present in Alzheimer's disease brains induce neurofibrillary tangle-like intracellular inclusions in neurons. *Proc. Natl Acad. Sci. USA*, **98**, 8838–8843.
38. Marques, M. A., Tolar, M., Harmony, J. A. & Crutcher, K. A. (1996). A thrombin cleavage fragment of apolipoprotein E exhibits isoform-specific neurotoxicity. *Neuroreport*, **7**, 2529–2532.
39. Cooper, T. & Woody, R. W. (1990). The effect of conformation on the CD of interacting helices: a theoretical study of tropomyosin. *Biopolymers*, **30**, 657–676.
40. Graddis, T. J., Myszka, D. G. & Chaiken, I. M. (1993). Controlled formation of model homo- and heterodimer coiled-coil polypeptides. *Biochemistry,* **32**, 12664–12671.
41. Lavigne, P., Kondejewski, L. H., Houston, M. E., Jr, Sönnichsen, F. D., Lix, B., Sykes, B. D. *et al.* (1995). Preferential heterodimeric parallel coiled-coil formation by synthetic max and c-myc leucine zippers: a description of putative electrostatic interactions responsible for the specificity of heterodimerization. *J. Mol. Biol.* **254**, 505–520.
42. Lazo, N. D. & Downing, D. T. (1997). Beta-helical fibrils from a model peptide. *Biochemistry,* **36**, 2559–2565.
43. Shotland, Y., Teff, D., Koby, S., Kobiler, O. & Oppenheim, A. B. (2000). Characterization of a conserved alpha-helical, coiled-coil motif at the C-terminal domain of the ATP-dependent FtsH (HflB) protease of *Escherichia coli*. *J. Mol. Biol.* **299**, 953–964.
44. Mehboob, S., Luo, B.-H., Patel, B. M. & Fung, L. W.-M. (2001). Alpha beta spectrin coiled-coil association at the tetramerization site. *Biochemistry*, **40**, 12457–12464.
45. Bode, K. A. & Applequist, J. (1997). Helix bundles and coiled-coils in alpha-spectrin and tropomyosin: a theoretical CD study. *Biopolymers*, **42**, 855–860.
46. Holtzer, M. E. & Holtzer, A. (1995). The use of spectral decomposition *via* the convex constraint algorithm in interpreting the CD-observed unfolding transitions of coiled-coils. *Biopolymers*, **36**, 365–379.
47. Clement-Collin, V., Leroy, A., Monteilhet, C. & Aggerbeck, L. P. (1999). Mimicking lipid-binding-induced conformational changes in the human apolipoprotein E N-terminal receptor-binding domain effects of low pH and propanol. *Eur. J. Biochem.* **264**, 358–368.
48. Kohn, W. D., Monera, O. D., Kay, C. M. & Hodges, R. S. (1995). The effects of interhelical electrostatic repulsions between glutamic acid residues in controlling the dimerization and stability of two-stranded α-helical coiled-coils. *J. Biol. Chem.* **270**, 25495–25506.
49. Hagihara, Y., Aimoto, S., Fink, A. L. & Goto, Y. (1993). Guanidine hydrochloride-induced folding of proteins. *J. Mol. Biol.* **231**, 180–184.
50. Monera, O., Zhou, N. E., Kay, C. M. & Hodges, R. S. (1993). Comparison of antiparallel and parallel two-stranded α-helical coiled-coils. *J. Biol. Chem.* **268**, 19218–19227.
51. Clark, A. C., Sinclair, J. F. & Baldwin, T. O. (1993). Folding of bacterial luciferase involves a non-native heterodimeric intermediate in equilibrium with the native enzyme and the unfolded subunits. *J. Biol. Chem.* **268**, 10773–10779.
52. Saito, H., Dhanasekaran, P., Nguyen, D., Baldwin, F., Weisgraber, K. H., Wehrli, S. *et al.* (2003). Characterization of the heparin binding sites in human apolipoprotein E. *J. Biol. Chem.* **278**, 14782–14787.
53. Grimsley, J. K., Scholtz, J. M., Pace, C. N. & Wild, J. R. (1997). Organophosphorus hydrolase is a remarkably stable enzyme that unfolds through a homodimeric intermediate. *Biochemistry,* **36**, 14366–14374.
54. Hornby, J. A. T., Codreanu, S. G., Armstrong, R. N. & Dirr, H. W. (2002). Molecular recognition at the dimer interface of a class mu glutathione transferase: role of a hydrophobic interaction motif in dimer stability and protein function. *Biochemistry,* **41**, 14238–14247.
55. Dergunov, A. D., Shuvaev, V. V. & Yanushevskaja, E. V. (1992). Quaternary structure of apolipoprotein E in solution: fluorimetric, chromatographic and immunochemical studies. *Biol. Chem. Hoppe-Seyler*, **373**, 323–331.
56. Dergunov, A. D., Vorotnikova, Y. Y., Visvikis, S. & Siest, G. (2003). Homo- and hetero-complexes of exchangeable apolipoproteins in solution and in lipid-bound form. *Spectrochim. Acta sect. A*, **59**, 1127–1137.
57. Forstner, M., Peters-Libeu, C., Contreras-Forrest, E., Newhouse, Y., Knapp, M., Rupp, B. & Weisgraber, K. H. (1999). Carboxyl-terminal domain of human apolipoprotein E: expression, purification, and crystallization. *Protein Expr. Purif.* **17**, 267–272.
58. Chothia, C., Levitt, M. & Richardson, D. (1977). Structure of proteins: packing of alpha-helices and pleated sheets. *Proc. Natl Acad. Sci. USA*, **74**, 4130–4134.
59. Narayanaswami, V. & Ryan, R. O. (2000). Molecular basis of exchangeable apolipoprotein function. *Biochim. Biophys. Acta*, **1483**, 15–36.
60. Laue, T. T. & Stafford, W. F., III (1999). Modern applications of analytical ultracentrifugation. *Annu. Rev. Biophys. Biomol. Struct.* **28**, 75–100.
61. Johnson, M. L., Correia, J. J., Yphantis, D. A. & Halvorson, H. R. (1981). Analysis of data from the analytical ultracentrifuge by nonlinear least-squares techniques. *Biophys. J.* **36**, 575–588.
62. Carr, C. M. & Kim, P. S. (1993). A spring-loaded mechanism for the conformational change of influenza hemagglutinin. *Cell*, **73**, 823–832.

Edited by M. F. Moody

(Received 10 July 2003; received in revised form 18 September 2003; accepted 22 September 2003)